ELSEVIER

Biophysical Chemistry 84 (2000) 137–147

Biophysical Chemistry

www.elsevier.nl/locate/bpc

Thermal activation of DNA frayed wire formation

Ekaterina Protozanova, Robert B. Macgregor Jr.*

Department of Pharmaceutical Sciences, Faculty of Pharmacy, University of Toronto, 19 Russell Street, Toronto, Ontario, M5S 2S2 Canada

Received 8 November 1999; received in revised form 20 December 1999; accepted 20 December 1999

Abstract

Dynamic light scattering has been used to study the formation of stable multistranded DNA complexes called frayed wires. DNA frayed wires arise from the indefinite self-association of oligonucleotides with long terminal tracks of guanines, e.g. $d(A_{15}G_{15})$. The complexes are stabilized via guanine–guanine interactions resulting in the formation of a guanine stem. Non-guanine portions of the oligonucleotide are disposed away from the stem and form single stranded arms. The indefinite nature of the self-association of these oligonucleotides leads to a distribution of aggregate molecular weights. The distribution arises from aggregated species that differ from one another by the number of self-associated oligonucleotides. In light-scattering experiments, the autocorrelation functions collected for frayed wires are bimodal. The slow mode, often observed for samples containing DNA and other polyelectrolytes, has been ascribed to the formation of large unspecific aggregates due to electrostatic or other long-range interactions. We attribute the fast mode to the translational diffusion of the polydisperse population in the frayed wire sample. We use the mean of the fast mode to characterize the growth of the frayed wires. Consistent with the gel electrophoresis studies, the aggregation of frayed wires is promoted by the presence of magnesium ions and incubation at high temperature. The rate of aggregate formation increases with temperature, indicating the positive activation energy for the reaction. We propose an energy diagram for the formation/disruption of frayed wires revealing the catalytic-like role of the complementary strand in the denaturation of high molecular weight complexes.

Keywords: Light scattering; Self-assembly; Multistranded DNA; Guanine-rich DNA; DNA frayed wires

* Corresponding author. Tel.: +1-416-978-7332; fax: +1-416-978-8511.
E-mail address: macgreg@phm.utoronto.ca (R.B. Macgregor)

0301-4622/00/$ - see front matter
PII: S0301-4622(00)00105-8

1. Introduction

DNA appears to hold considerable potential for the fabrication of nanometer-scale structures. The manufacture and characterization of these structures have attracted considerable interest [1–4]. Recently, Seeman and coworkers described the formation of large ordered two-dimensional aggregates by annealing two or more types of DNA double-crossover molecules [4]. Monomeric units arrange themselves in a regular array with defined periodicity. When probed with atomic force microscopy, the aggregates appear as stripes of matter reaching up to several microns in length. The high specificity of the non-covalent interactions between complementary sequences and the ability of DNA to adopt a variety of different conformations enable the design and manufacture of structures with stringently defined geometry. In addition, the formation of a double or triple helix involves only non-covalent interactions, proceeding without enzyme or catalyst. Thus, these structures are self-assembling.

Another class of self-assembling DNA superstructures arises from the mutual non-covalent interaction that occurs between guanine-rich oligonucleotides. Guanine–guanine interactions mediate the association of multiple strands of $d(G_4T_2G_4)$ into long, rod-like entities, called G-wires [5]. We have reported that oligonucleotides with long terminal tracks of guanines, e.g. $d(A_{15}G_{15})$, self-associate to form extremely stable multistranded complexes, which we call DNA frayed wires [6,7]. When resolved by native and denaturing gel electrophoresis, DNA frayed wires appear as a ladder of discrete, regularly spaced bands (Fig. 1). The aggregates, represented on the gel as bands with mobilities lower than that of the monomer, arise from guanine–guanine interactions. We refer to this part of the frayed wire structure as the *guanine stem*. Non-guanine portions of the parent strands project from the stem and form *single-stranded arms*. The two domains within the frayed wire are structurally and thermodynamically independent [8]. When visualized by atomic force microscopy frayed wires appear as elongated entities reaching up to 100 nm in length (unpublished data).

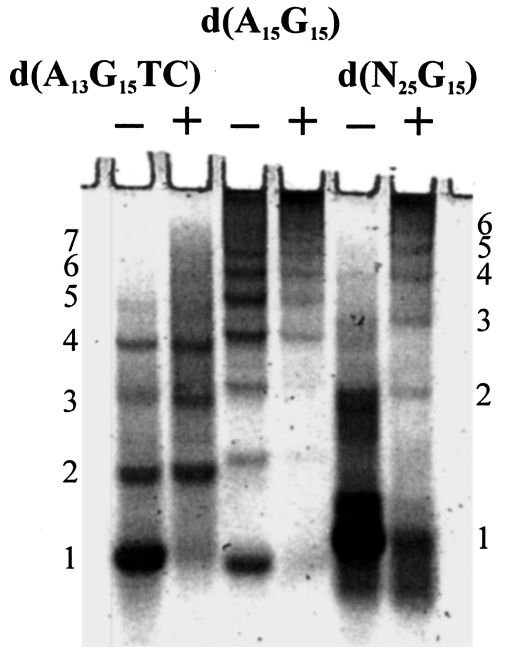

Fig. 1. Polyacrylamide gel electrophoresis of frayed wires of $d(A_{15}G_{15})$ and $d(N_{25}G_{15})$ generated by incubation at 80°C for 30 min in the presence of 5 mM $MgCl_2$ (lanes marked '+') are compared with the samples without heating (lanes marked '–'). Also shown are the complexes formed by $d(A_{13}G_{15}TC)$. The band with the highest mobility in each lane corresponds to the monomer, slower migrating species result from the association of parent oligonucleotides. The number of parent strands in the aggregates of $d(A_{15}G_{15})$ and $d(N_{25}G_{15})$ are shown to the left and to the right of the gel, respectively.

In this contribution, we describe the use of dynamic light scattering (DLS) to study the formation of DNA frayed wires. Dynamic light scattering is useful for the characterization of the structure and dynamics of biological macromolecules including double stranded DNA of different sizes. The dynamic light scattering signal arises from the fluctuations in the concentration of scattering centers, in our case a macromolecule, in the laser light beam. The fluctuations are related to the rate of diffusion of the macromolecule in and out of the light path. The time decay of the similarities in the fluctuations (correlation function) of the light scattered when passing through a medium containing scattering centers is collected in the DLS experiments. Therefore, measurement of the autocorrelation

permits one to calculate characteristics related to the dynamics of the scattering centers, such as the diffusion coefficient, size and shape of the macromolecules.

The group of Pecora [9–11] has performed a comprehensive DLS study over a wide range of sizes of DNA. This includes 2.3 kbp superhelical DNA, sonicated low molecular weight DNA fragments of 150–250 bp and a synthetic 20-bp duplex. Under certain conditions, the autocorrelation functions of DNA samples are bimodal. The fast mode arises from the collective diffusion of the molecules. This mode has distinct diffusive characteristics and has been ascribed to the translational motion of individual chains in the solution. In the current literature, the presence of the slow mode in the solutions of DNA and other polyelectrolytes is most often attributed to the transient formation of multi-chain aggregates due to electrostatic interactions at low salt or high polyelectrolyte concentration. However, the origin of the slow mode remains uncertain, and other explanations have been advanced [12,13].

Here we use dynamic light scattering to characterize a multidisperse population of frayed wires formed via association of different numbers of the parent oligonucleotide. We explore the effect of the salt conditions and temperature on the extent and kinetics of aggregation. We propose an energy diagram for the self-association/denaturation of frayed wires and speculate about the catalytic role of the complementary strand in the disruption of the aggregates.

2. Experimental

2.1. DNA

We purchased the oligodeoxyribonucleotides, $d(A_{15}G_{15})$, $d(C_{15}T_{15})$, $d(A_{13}G_{15}TC)$, d(ATCACGCTTTTGTTCCTGATGAAAAG$_{15}$), denoted as $d(N_{25}G_{15})$, from the HSC Biotechnology Service Centre at the University of Toronto, Canada. Lyophilized DNA was resuspended in water at a final concentration of 4 mg/ml and stored at −20°C. For dynamic light-scattering experiments, samples with a total volume of 1.5 ml were prepared by mixing 150 μl of the DNA stock solution in 10 mM Tris–HCl (pH 8.0) buffer containing 1 or 5 mM $MgCl_2$. The samples were heated to 95°C and cooled slowly to room temperature followed by incubation at 4°C. Alternatively, freshly prepared diluted samples were used directly without heating to study the temperature-induced formation of the frayed wires. Solutions of oligonucleotides were passed through 0.22-μm Millex®-GP filters (Millipore, Bedford, MA, USA) immediately prior to the light-scattering experiment.

2.2. Dynamic light scattering

Dynamic light-scattering experiments were performed using a laser light-scattering photometer (Brookhaven Instruments Corp., Redditch, UK). Light source was a Lexel Excel 3000 Argon-ion laser operating at wavelength of 514.5 nm using the power range of 0.3–1.5 W. Samples in a glass scattering cell were placed into a thermostated cell holder of a BI-200SM goniometer. The cell holder was filled with toluene to match the index of refraction of the glass scattering cell. If not stated otherwise, the measurements were performed at 20°C. The light scattered at 90° to the incident beam was detected with a photomultiplier interfaced to the 136-channel BI-2030AT digital correlator.

The underlying distributions of decay times were obtained by fitting the experimentally determined intensity autocorrelation functions using GENDIST. This routine uses a model-free fitting algorithm, there is no presupposed form describing the distribution of relaxation times. Characteristic decay times for different modes, τ_r, and their relative amplitudes were acquired by analysis of the moments of distribution functions. Diffusion coefficients, D, were calculated from $D = (1/\tau_r)q^{-2}$, where $q = (4\pi n/\lambda_0)\sin(\theta/2)$ is the scattering vector, n is the refractive index of the solution, λ_0 is laser wavelength, and θ is the scattering angle. The hydrodynamic diameter, a, associated with the given mode was calculated to facilitate the comparison of the samples at different temperatures, according to $a = k_B T/3\pi\eta D$, where T is the absolute temperature, and η is the solvent viscosity. The values of the refrac-

tive index of water and the water viscosity tabulated in the *CRC Handbook of Chemistry and Physics* [14] for different temperatures were used to account for the temperature dependence of n and η.

2.3. Native gel electrophoresis

Freshly prepared solutions of the oligonucleotides in 10 mM Tris–HCl (pH 8.0) 5 mM $MgCl_2$ were subjected to high-temperature incubation using GeneAmp® PCR System 2400 (Perkin-Elmer, Norwalk, CT, USA). The samples with a total volume of 7 μl were 20 μM in strands. The products resulting from the incubation were resolved by electrophoresis in 2.8% agarose gels or 10% polyacrylamide gels with TBE (90 mM Tris–borate and 2 mM EDTA) as a running buffer. After the completion of electrophoresis, the gels were stained in 100 ml of 1× SYBR® Gold nucleic acid gel stain (Molecular Probes, Eugene, OR, USA). The band patterns were visualized by illuminating the gel with 312-nm light from a transilluminator. A 20-bp ladder (Sigma, St. Louis, MO, USA) was used as a molecular weight marker.

2.4. Denaturing gel electrophoresis

Approximately 100 pmol of $d(A_{15}G_{15})$ was 5′-end labeled with [γ-^{32}P]ATP using T4 polynucleotide kinase (Pharmacia). The samples of frayed wires were prepared by mixing 10 pmol of the unlabelled $d(A_{15}G_{15})$ with approximately 1 pmol of radiolabelled oligonucleotide in 90 mM Tris–borate (pH 8.3) buffer containing 5 mM $MgCl_2$. The mixture was heated to 90°C and then slowly cooled to 4°C followed by a 15-h incubation at this temperature. The samples with the total volume of 5 μl were then placed in a water bath at the desired temperature. After the addition of 20 pmol of $d(C_{15}T_{15})$, the samples were incubated for 2 h. The volume of the control samples, to which no complementary strands had been added, was adjusted by addition of an appropriate amount of water. The products were resolved using electrophoresis in 10% denaturing polyacrylamide gels run at 50°C. The gels were dried under vacuum at 80°C. Digital images of the band patterns were collected using an Ambis model 4000 radioanalytic imaging system (Scanalytics, Inc., Bellerica, MA, USA).

3. Results

3.1. Distribution of decay times is bimodal

Intensity correlation functions collected for solutions of $d(A_{15}G_{15})$ frayed wires annealed in the presence of magnesium ions significantly deviate from a single exponential decay. As shown in Fig. 2a, non-random residuals are obtained from a single exponential fit while random and small residuals result from a two exponential fit. The underlying distributions of decay times obtained using GENDIST are bimodal (Fig. 2b).

The slow component in the correlation functions collected for the solutions of DNA and other polyelectrolytes has been observed previously by other investigators [9–13]. It is usually attributed to the dynamics of large transient multi-chain domains of polyelectrolytes arising from electrostatic or other long-range interactions. The amplitude of the slow component is greatly favored by low ionic strength and high DNA concentration. It has also been suggested that the appearance of the slow mode for polydisperse DNA samples is not entirely due to the electrostatic interactions, but may also arise from the interparticle diffusion in a polydisperse population of species [12].

In our experiments, the hydrodynamic diameter associated with the slow mode varies from 100 to 140 nm for different samples. This is similar to the sizes of the structures attributed to the slow mode in other studies in which no self-aggregation was suspected [11,13]. The amplitude of the slow mode depends strongly on the salt conditions of the solution; the fraction of the slow mode decreasing with increasing ionic strength (Fig. 2b). In addition, the relative amount of the species contributing to the slow mode decreases upon heating the sample suggesting that they ‘melt’ at high temperatures (Fig. 4a). Although ionic strength and temperature affect the amplitude of

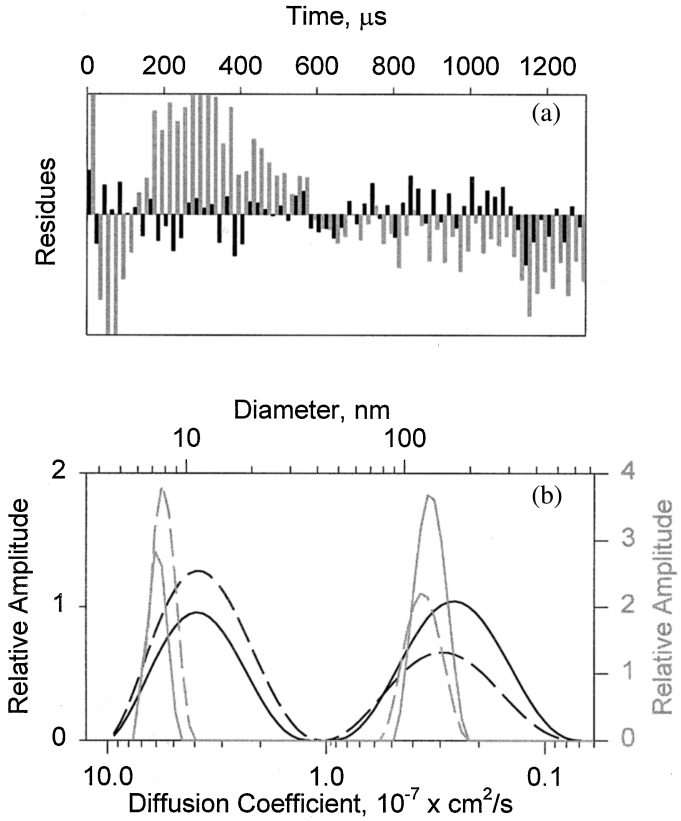

Fig. 2. (a) Residual plots for the correlation function fitted to a single exponential (gray) and double exponential decays (black). The correlation function was collected at 20°C for the $d(A_{15}G_{15})$ frayed wires annealed in the presence of 1 mM $MgCl_2$. (b) Underlying distributions of relaxation times for $d(A_{15}G_{15})$ (black) and $d(A_{13}G_{15}TC)$ (gray) are compared under different salt conditions. The samples were annealed in the presence of 5 mM $MgCl_2$ (solid lines) followed by addition of NaCl to a final concentration of 600 mM (dashed lines). Note the twofold difference in the vertical scales for $d(A_{15}G_{15}TC)$ (right) and $d(A_{15}G_{15})$ (left).

the slow mode, it is present even at the highest salt concentrations and temperatures employed in our study.

We interpret the fast mode as arising from the translational diffusion of frayed wires. The frayed wire sample is a polydisperse population of complexes originating from the association of various numbers of parent strands; the resulting aggregates differ in molecular weight and size. We are unable to distinguish between different species present in the sample of frayed wires, i.e. parent strand monomers, and the products of association of the monomers. We have used the relaxation time of the fast mode to characterize the whole population of frayed wires.

3.2. Aggregate formation by $d(A_{15}G_{15})$ and $d(A_{13}G_{15}TC)$

We have shown before that the presence of several consecutive terminal guanines is essential for the ability of an oligonucleotide to associate into frayed wires [6]. When non-guanine bases are added to the 3′-end of the parent strand, e.g. $d(A_{13}G_{15}TC)$, only complexes consisting of two, three, and four stands are formed (Fig. 1). There is no further polymerization. The distributions of relaxation times for $d(A_{13}G_{15}TC)$ and frayed wires of $d(A_{15}G_{15})$ are compared in Fig. 2b. The distribution for the $d(A_{13}G_{15}TC)$ sample is bimodal; the half-width of both modes is much smaller

than that of the d($A_{15}G_{15}$) frayed wires. This is consistent with the failure of d($A_{13}G_{15}$TC) to aggregate into high molecular weight species, therefore the population of the higher order structures, and the polydispersity of the sample, is smaller. Increasing the NaCl concentration to 600 mM affects the relative amplitude of the fast and slow modes without changing the position of the maxima. As expected, the fraction of the slow mode decreases with salt concentration for both samples (Fig. 2b).

3.3. The effect of temperature on frayed wire formation

We conducted a series of experiments to study the effect of temperature on the state of aggregation of frayed wires and to explore the stability of the species contributing to the slow mode. For these experiments, a freshly prepared solution of the parent oligonucleotide, d($A_{15}G_{15}$) or d($N_{25}G_{15}$), in Tris–HCl buffer (pH 8.0) containing 5 mM $MgCl_2$ was immersed in the sample chamber connected to a water bath. The temperature was gradually increased to 64°C. The sample was incubated at this temperature for 20 min before slow cooling to 20°C. Intensity correlation functions were collected at different temperatures. The apparent sizes of the frayed wires were calculated from the characteristic decay times of the fast mode at each temperature (Fig. 3a). Frayed wires arising from d($A_{15}G_{15}$) and d($N_{25}G_{15}$) exhibit identical behavior. The apparent size of the aggregates increases somewhat with incubation time at 64°C. Further growth stops when the temperature is lowered. After this treatment, the average size for both samples reaches approximately the same value, 14 nm. Evidently, we are observing the temperature-induced initiation of frayed wire formation. Polymerization is strongly favored by the elevated temperature and it slows dramatically when the temperature is decreased.

As expected, d($A_{13}G_{15}$TC) does not exhibit significant growth under the same experimental conditions. The apparent size of the complexes formed by this oligonucleotide fluctuates between 6 and 7 nm following heating, incubation at 64°C, and cooling. This is consistent with the gel electrophoretic data showing that d($A_{13}G_{15}$TC) fails to form high molecular weight aggregates, emphasizing again the importance of terminal guanines in the frayed wire structure.

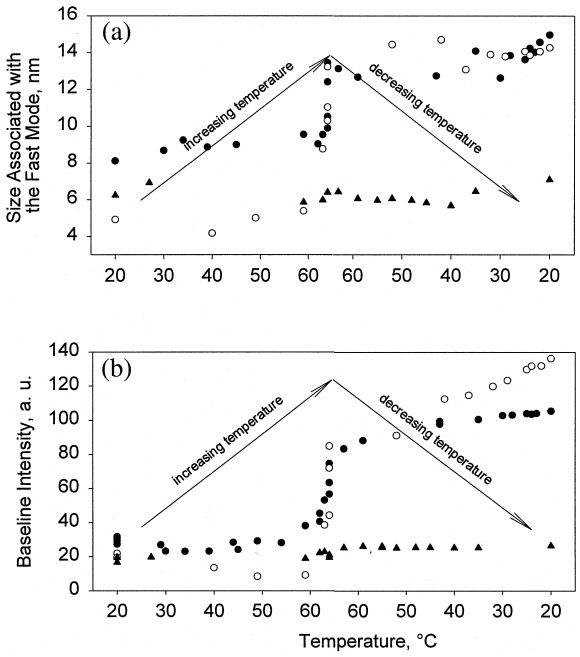

Fig. 3. The effect of temperature on the aggregation of d($A_{15}G_{15}$) (closed circles), d($N_{25}G_{15}$) (open circles) and d($A_{13}G_{15}$TC) (triangles). Dependence of the size associated with the fast mode (a) and the intensity of the baseline of the correlation function (b) on the temperature. Freshly prepared samples of parent oligonucleotides containing 5 mM $MgCl_2$ were heated to 64°C, followed by a 20-min incubation at this temperature and slow cooling to 20°C.

We also explored the time dependence of the baseline of the correlation functions. The baseline intensity is equivalent to the intensity of the static light-scattering signal and is related to the extent of the aggregate formation in the sample. As expected, the baseline intensity exhibits the same temperature dependence as the apparent size of frayed wires described above (Fig. 3b). This indicates again the temperature-induced formation of large species by oligonucleotides with terminal runs of guanines, d($A_{15}G_{15}$) and d($N_{25}G_{15}$), in contrast to d($A_{13}G_{15}$TC), which does not polymerize under the same conditions.

3.4. Temperature-induced initiation of frayed wire formation

We followed the time course of frayed wire formation by placing a freshly prepared solution of $d(A_{15}G_{15})$ into the cell chamber at 64 and 81°C. The size distributions obtained at different time points after the initiation of the association at 64°C are compared in Fig. 4a. Firstly, the fraction of slow mode decreases from 80% to 25% of the total intensity at 20 and 64°C, respectively. This is consistent with the disruption of large unspecific aggregates at the higher temperature. Secondly, there is a clear tendency for growth of the aggregates indicated by an increase in the mean and the amplitude of the fast mode. The size associated with the frayed wires in this experiment changed from 7.3 nm for the $d(A_{15}G_{15})$ sample before heating to 28 nm 150 min after increasing the temperature.

In addition to the changes in the hydrodynamic size of the frayed wires with time, the baseline of the correlation functions also increases. The time evolution of baseline amplitude collected at 64°C and 81°C is presented in Fig. 4b. Note the 20-fold difference in the ordinate scale for the two conditions. At both temperatures, the amplitude increases in an apparently hyperbolic manner with

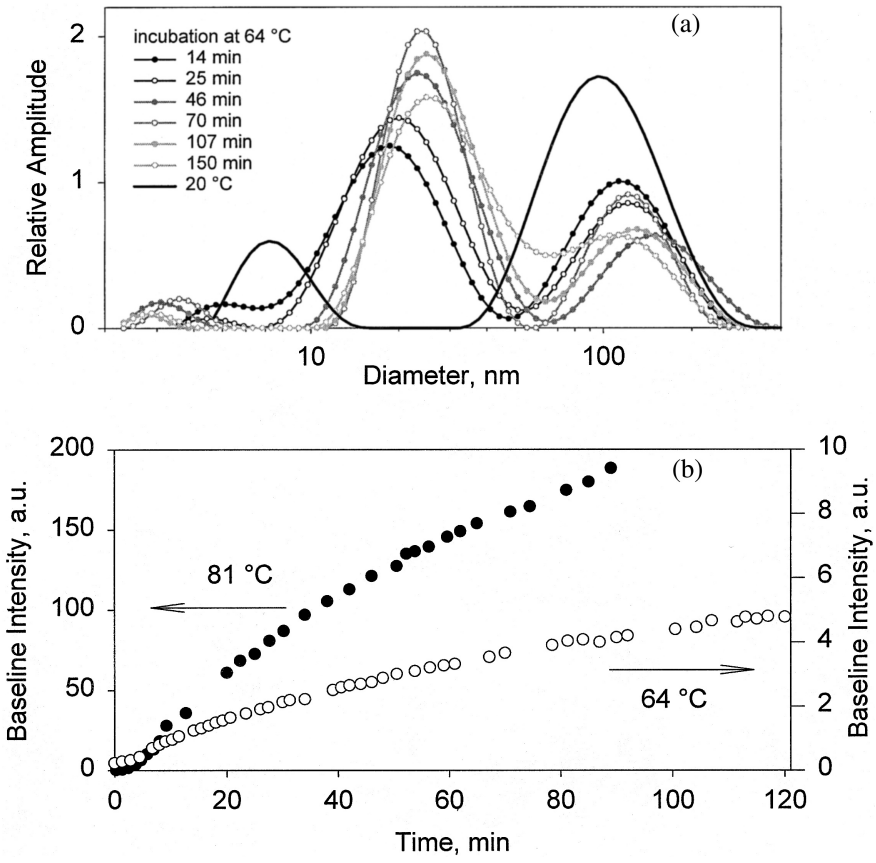

Fig. 4. (a) The time evolution of the size distribution for $d(A_{15}G_{15})$ in 5 mM $MgCl_2$ following the initiation of aggregation by heating to 64°C. Also shown is the size distribution collected at 20°C before the start of the reaction (—). (b) The time course of the temperature-induced association of $d(A_{15}G_{15})$. Frayed wire formation was initiated by heating a freshly prepared sample of $d(A_{15}G_{15})$ in 5 mM $MgCl_2$ to 64°C (○) and 81°C (●). The kinetics of aggregation were monitored following the intensity of the correlation function baseline at different times after initiation of the reaction. Note there is a 20-fold difference in the ordinate scale for the two experiments.

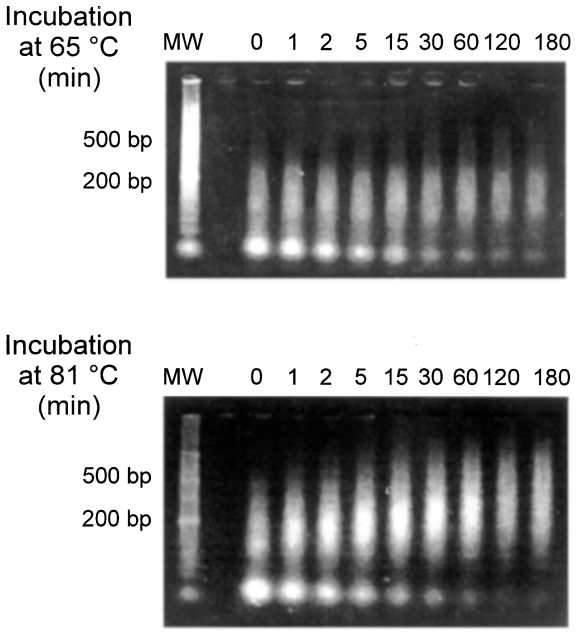

Fig. 5. The time evolution of frayed wire formation by $d(A_{15}G_{15})$ following incubation in the presence of 5 mM $MgCl_2$ at 64°C and 81°C, as resolved by agarose gel electrophoresis. Incubation at elevated temperature for longer time results in a higher degree of aggregation, which appears on the gel as a smear with a limited mobility. The time of incubation is indicated at the top of each lane. The sample in the leftmost lane is a 20-bp molecular weight ladder; intense bands correspond to 200- and 500-bp fragments.

time, within the timeframe of our experiments the reaction does not reach equilibrium under either condition. We conclude that aggregation is promoted by high temperature, and that the activation energy of frayed wire formation is positive.

The time course of the aggregation can also be observed by electrophoresis in agarose gels (Fig. 5). Longer incubation at 64°C leads to redistribution of the strands from the band corresponding to monomers to their aggregates, which appear on this gel as a smear with reduced mobility. Incubation at 81°C results in a greater degree of polymerization; the smear extends towards complexes with lower mobility indicative of the formation of larger structures.

3.5. Denaturation of frayed wires

One of the characteristic features of frayed wires is their extreme stability towards thermal denaturation. Although only non-covalent interactions are involved in the stabilization of the complexes, the high-molecular weight aggregates are still present in the patterns of the electrophoresis gels run under denaturing conditions (7 M urea, 55°C) [6]. Despite this stability, the $d(A_{15}G_{15})$ frayed wires are easily disrupted in the presence of the complementary strand. Incubation of preformed frayed wires with $d(C_{15}T_{15})$ leads to the formation of a Watson–Crick duplex which when resolved by electrophoresis on native gels appears as an intense band with a mobility lower than that of the monomer. As expected this duplex is readily denatured and only the band corresponding to the monomer is present in the lanes following the incubation with the complementary strand.

We have proposed that the interaction of the complementary strand with the frayed wire initially involves the hybridization of the of the thymine runs of $d(C_{15}T_{15})$ to the adenine arms of frayed wires [6]. Then the duplex propagates in the direction of the stem destabilizing the guanine–guanine interactions and disrupting the complex. Since the initial interaction involves the folding of a standard Watson–Crick duplex we expect this process to exhibit negative activation energy, i.e. disruption of the aggregates to be favored by low temperatures. We tested this hypothesis by monitoring the extent of the reaction (disruption of high molecular weight aggregates) at four different temperatures (Fig. 6). Preformed $d(A_{15}G_{15})$ frayed wires were incubated in the presence of the complementary strand and the sample was resolved under denaturing conditions. The typical ladder pattern of frayed wires is still present in the lanes corresponding to the sample after high-temperature incubation (64°C and 80°C) while the complexes disappear following incubation at lower temperatures (25°C and 37°C). This temperature range is consistent with the stability of the $d(A_{15})$:$d(T_{15})$ duplex under the conditions used in our experiments. We previously reported the midpoint of the thermal denaturation of the complex formed between the arms of $d(A_{15}G_{15})$ frayed wires and dT_{15} to be 46°C [8]. Hybridization of the thymine runs of $d(C_{15}T_{15})$ to

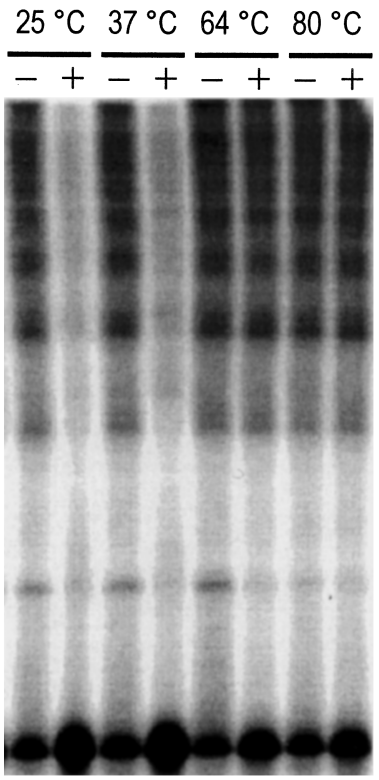

Fig. 6. The effect of temperature on the disruption of preformed frayed wires in the presence of the complementary strand (lanes marked '+'). The samples of ^{32}P-labeled $d(A_{15}G_{15})$ frayed wires were resolved on denaturing gels following 2 h incubation with $d(C_{15}T_{15})$ at the temperatures indicated at the top of the gel. Lanes marked '−' are controls with no complementary strand added.

the arms readily proceeds at the temperatures below the melting point of the duplex followed by propagation of the duplex towards the stem and disruption of aggregates. However, the nucleation is hindered at elevated temperatures and frayed wires remain intact.

4. Discussion

4.1. Formation of frayed wires exhibits positive activation energy

Formation of DNA frayed wires is an example of an indefinite self-association. The monomers, or parent oligonucleotides, aggregate into species of infinitely growing stoichiometry as opposed to the closed self-association when the oligomerization is restrained to a certain number of structures, e.g. dimers, trimers. A consequence of open self-association is that the sample contains species of a wide range of molecular weights and sizes. The characterization of these complex polydisperse systems poses problems in terms of their analytical description and the choice of an experimental technique. Sedimentation velocity and dynamic light-scattering experiments are both valuable techniques for the characterization of indefinite self-associating systems. Analytical ultracentrifugation has been used to study the open self-association of guanine dinucleotides and similar systems [15,16].

We report the use of DLS to assess the apparent size of DNA frayed wires and the temperature dependence of the self-association process. DNA frayed wires are aggregates arising from the interaction of several strands of guanine-rich oligonucleotides. Since each sample contains species composed of different number of parent strands, i.e. monomers, dimers, and higher-order aggregates, the sample presents a polydisperse population of complexes differing in molecular weights and sizes. We assume that the fast component of the bimodal distribution of decay times arises from the translational diffusion of all types of aggregates present in the sample. We use the characteristic decay time of the fast mode to estimate the apparent size associated with the whole population of the frayed wires. The calculated hydrodynamic diameter of the frayed wires ranges from 5 to 28 nm depending on the history of the sample and salt conditions.

We have shown that upon high-temperature incubation, magnesium-containing samples exhibit a notable increase in the apparent size. The same trend is observed for the intensity collected from the baseline of the correlation functions; the intensity increases with time and temperature. As resolved by electrophoresis in agarose gels, frayed wires tend to grow into larger aggregates when incubated at higher temperature confirming that the reaction of frayed wire formation is favored by elevated temperature. Consequently, the rate and the extent of aggregate formation increase

with heating, consistent with a positive activation energy for this reaction. This behavior is atypical for nucleic acids; helix formation reactions often exhibit negative activation energies for the formation of double and triple helical structures [17,18].

There are several possible ways to rationalize the positive activation energy observed for frayed wire formation. It may indicate the presence of stable secondary structure within the arms or the stem of the complexes that hinder the association of high molecular weight superstructures at low temperatures. These interactions are disrupted upon heating allowing the polymerization of the parent strand to proceed. It is also possible that the addition of another strand to a preformed frayed wire requires the 'opening' of an existing structure to make it more accessible for the newly introduced strand. We are presently unable to attribute our observations to either of these, or other, possibilities.

The oligonucleotide $d(N_{25}G_{15})$, adopts a stable secondary structure at room temperature. When resolved by non-denaturing gel electrophoresis, there are two species present, a monomer and a dimer (Fig. 1). There is no indication of further polymerization. Most likely these species correspond to a hairpin and a duplex. In both cases, the formation of the secondary structure interferes with the guanine track of the oligonucleotide completely precluding it from aggregate formation. These putative structures are destabilized at high temperatures and polymerization then occurs.

4.2. Energetics of frayed wire formation

In Fig. 7 we propose an energy diagram for the formation and disruption of frayed wires. Dynamic light scattering experiments show that the rate of formation of large multistranded aggregates is favored by high temperature indicating a positive activation energy for the reaction (**1**). Once formed, frayed wires are resistant towards standard denaturation conditions and appear as a regular ladder pattern of bands after electrophoresis on denaturing gels. However, these

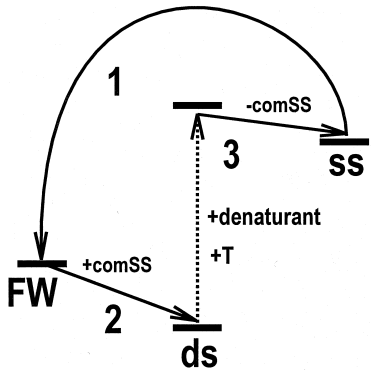

Fig. 7. A catalytic-like role of the complementary strand in the denaturation of frayed wires. Self-association (**1**) of the parent single strands (ss) into frayed wires (FW) exhibits a positive activation energy. Complexes are extremely stable and are resistant towards standard denaturation conditions. However, frayed wires are disrupted spontaneously (**2**) following low-temperature incubation in the presence of the complementary strand (comSS). This leads to the formation of a duplex (ds). The duplex in turn is denatured (**3**) upon heating in the presence of denaturant. The complementary strand plays a catalytic-like role by lowering the energetic barrier of frayed wire denaturation by the formation of a duplex DNA intermediate. The cartoon is a schematic; it is not intended to show any specific details, rather to outline the pathways involved in the process.

complexes are spontaneously disrupted upon addition of the complementary strand (**2**) leading to the formation of Watson–Crick duplex [6]. Since the interaction of the complementary strands with the frayed wires initially involves the formation of a standard duplex with the arms the process of the 'complementary strand-assisted' denaturation of frayed wires is favored by low temperature. The reaction proceeds readily at the temperatures below the midpoint of thermal denaturation of the complex formed with the arms.

The pathway for disruption of frayed wires, depicted in Fig. 7, involves two steps. Low-temperature incubation of DNA frayed wires in the presence of the complementary strand results in the formation of a duplex intermediate (**2**). If the duplex is heated or if a denaturant (urea, formamide) is added to the solution, the duplex is denatured and the complementary strand is released (**3**). The role of the complementary strand in the disassembly of frayed wires is similar to the

action of a catalyst. This analogy arises from the formation of an intermediate complex, double-stranded DNA, with a reactant that lowers the energetic barrier for the denaturation. Recently, DNA oligonucleotides have been shown to catalyze the strand displacement reaction between two complementary strands one of which is initially hybridized to a protective strand [19]. The protective strand is designed so that one of the reactants is a double-stranded complex with a 40-base loop in the middle. Although displacement of a protective strand with a fully complementary strand is energetically favorable, the initiation of the reaction is inhibited due to geometrical constraints within the unpaired region in the loop, which preclude the twisting of the complementary strands around each other. However, the displacement reaction is catalyzed by opening the loop upon hybridization of a short oligonucleotide complementary to one of the arms of the initial complex. The catalytic role attributed to the short oligonucleotide in this system is analogous to the action of the complementary strand in the reaction of frayed wire denaturation.

Acknowledgements

This work was supported in part by grants from NSERC and Glaxo Wellcome Canada to R.B.M., and an Ontario Graduate Scholarship to E.P.

References

[1] N.C. Seeman, Angew. Chem. 37 (1998) 3220–3238.
[2] T.W. Nilsen, J. Grayzel, W. Prensky, J. Theor. Biol. 187 (1997) 273–284.
[3] T. Horn, M.S. Urdea, Nucl. Acids Res. 17 (1989) 6959–6967.
[4] E. Winfree, F. Liu, L.A. Wenzler, N.C. Seeman, Nature 394 (1998) 539–544.
[5] T.C. Marsh, E. Henderson, Biochemistry 33 (1994) 10718–10724.
[6] E. Protozanova, R.B. Macgregor, Jr., Biochemistry 35 (1996) 16638–16645.
[7] K. Poon, R.B. Macgregor, Jr., Biopolymers 45 (1998) 427–434.
[8] E. Protozanova, R.B. Macgregor, Jr., Biophys. J. 75 (1998) 982–989.
[9] J. Seils, R. Pecora, Macromolecules 28 (1995) 661–673.
[10] H.Tj. Goïnga, R. Pecora, Macromolecules 24 (1991) 6128–6138.
[11] L. Skibinska, J. Gapinski, H. Liu, A. Patkowski, E.W. Fischer, R. Pecora, J. Chem. Phys. 110 (1999) 1794–1800.
[12] M.E. Ferrari, V.A. Bloomfield, Macromolecules 25 (1992) 5266–5276.
[13] M. Sedlák, J. Chem. Phys. 105 (1996) 10123–10133.
[14] CRC Handbook of Chemistry and Physics, 61st ed., CRC Press Inc., Boca Raton, 1980/1981, pp. E-391, F-51.
[15] J. Behlke, O. Ristau, Eur. Biophys. J. 25 (1997) 325–332.
[16] C. Walss, B. Demeler, J.C. Hansen, L.A. Walmsley, J. Biomol. Struct. Dyn. 14 (1997) 898.
[17] D. Pörschke, M. Eigen, J. Mol. Biol. 62 (1971) 361–381.
[18] M.E. Craig, D.M. Crothers, P. Doty, J. Mol. Biol. 62 (1971) 383–401.
[19] A.J. Turberfield, B. Yurke, A.P. Mills Jr., DIMACS Series in Discrete Mathematics and Theoretical Computer Science (1999) in press.